Polar structures of bent-core liquid crystals with tetrathiafulvalene units

I. Alonso,[1] J. Martínez-Perdiguero,[1] C. L. Folcia,[1] J. Etxebarria,[1] J. Ortega,[2] I. C. Pintre,[3] and M. B. Ros[3]
[1]*Departamento de Física de la Materia Condensada, Facultad de Ciencias, Universidad del País Vasco, Apartado 644, 48080 Bilbao, Spain*
[2]*Departamento de Física Aplicada II, Facultad de Ciencias, Universidad del País Vasco, Apartado 644, 48080 Bilbao, Spain*
[3]*Química Orgánica, Facultad de Ciencias–Instituto de Ciencia de Materiales de Aragón, Universidad de Zaragoza—CSIC, 50009 Zaragoza, Spain*
(Received 5 May 2008; published 1 October 2008)

We report on a series of three bent-core liquid crystals containing tetrathiafulvalene units. Their characterization consisted of electro-optical observations, second-harmonic generation (SHG) analysis, and x-ray diffraction measurements. Compound I exhibits a lamellar optically isotropic phase on cooling from the isotropic liquid and undergoes a nonreversible field-induced transition to a birefringent state. The two others present two-dimensional structural periodicities, being only compound II switchable. Additionally, the electron density maps of compounds II and III have been obtained based on the analysis of the x-ray diffraction intensities. According to SHG measurements the ground state is antiferroelectric in the three compounds. A quite good SHG performance is found in compounds I and II.

DOI: 10.1103/PhysRevE.78.041701 PACS number(s): 61.30.Cz, 61.05.cf

I. INTRODUCTION

Since the discovery of achiral bent-core mesogens (or banana-shaped liquid crystals) [1], these materials have raised great expectations in the field of ferroelectric liquid crystals. Increasing basic research is motivated mainly by their capability to order into a wide variety of chiral and polar structures, as well as promising nonlinear optical properties [2,3]. Among them, the B_2 phase (SmCP) is the most extensively studied. However, apart from lamellar arrangements, others are also found, such as columnar, undulated, and modulated. From the structural point of view, the determination of the molecular organization is a challenge itself because there is no straightforward method. This is even more difficult when peculiar distributions arise at mesoscopic levels, as is the case, for instance, of the so-called dark conglomerate and racemate phases. The origin of this fascinating feature appearing in some bent-core mesophases is not totally understood yet, and several possibilities have been proposed: steric reasons, escape from polarization, and conformational chirality [4].

Another challenging issue is related to the molecular design. The mesomorphic properties of this kind of materials present a high sensitivity to chemical structure modifications giving rise to new interesting properties. In this respect, great efforts are being made on synthesizing materials with specific mesophases and features by using different molecular geometries and proper functional groups. Here we analyze three bent-core structures containing tetrathiafulvalene (TTF) units. TTF and its derivatives are very well-known due to their intermolecular charge transfer properties and are usually employed in molecular electronics as organic conductors and semiconductors [5–8]. Their interest also lies in the fact that inside a molecule they behave as good electron donors [5]. Hence this property can be useful for the development of materials with good nonlinear optical properties, like second harmonic generation (SHG).

In this work we report the characterization study of three different bent-core liquid crystals with TTF units. Based on electro-optical, x-ray scattering, and SHG measurements, we elucidate the structure and some properties of the mesophases. Furthermore, their capabilities as nonlinear optical materials are estimated.

II. EXPERIMENT

The chemical structures and phase sequences of the studied materials on cooling are shown in Fig. 1. The synthesis and some preliminary characterization data have been published elsewhere [9]. The phase assignment will be discussed separately for each mesogen below. As can be seen, compound III has one TTF unit next to the terminal chain in both lateral structures of the molecule whereas compounds I and II possess only one TTF unit.

For the characterization study, we first analyzed the optical textures and electro-optical behavior by polarized light microscopy. Samples were prepared in commercially available cells (Linkam) of 5 μm nominal thickness, in which an electric field can be applied perpendicular to the glass substrates. SHG measurements were carried out in the same cells. The measurements were performed with an experimental setup described in detail elsewhere [10]. The fundamental light is a Q-switched Nd-YAG laser (wavelength 1064 nm) with a pulse width of 6 ns and a frequency of 5 Hz. A square-wave electric field synchronized with the laser pulse was applied to the sample. X-ray measurements on nonoriented samples were also performed using a small-angle goniometer equipped with a high-temperature stage and a linear position-sensitive detector (PSD) with 4° of angular range. In order to check the liquid crystalline character of the phases, we employed a wide-angle goniometer of similar features. Monochromatic Cu Kα radiation was used. The materials were introduced in the isotropic phase into Lindemann capillaries with 0.5 mm diameter.

III. RESULTS AND DISCUSSION

A. Compound I

This material shows a completely dark texture, indistinguishable from the isotropic liquid, down to room tempera-

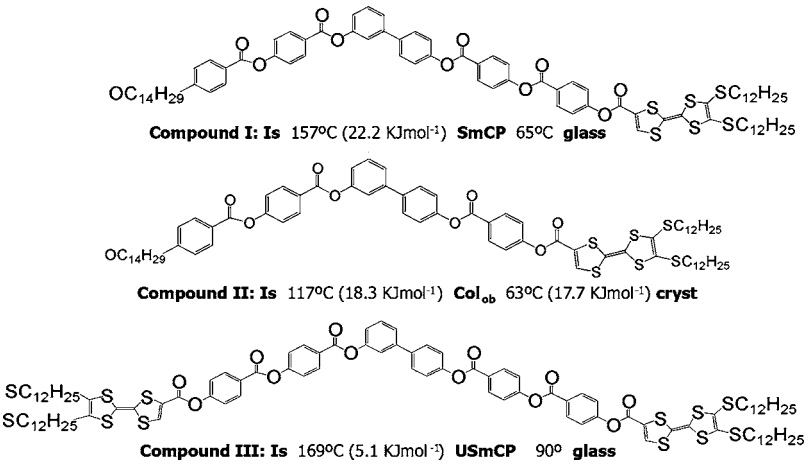

FIG. 1. Chemical structure of the compounds I, II, and III, together with their phase sequence and enthalpies on cooling. The transition temperatures were obtained from differential scanning calorimetry.

ture on cooling from the isotropic phase. The x-ray diffraction pattern shows two peaks, which correspond to the first and second orders of a given periodicity. A diffuse peak is also observed at wide angles, which confirms the mesomorphic character of the phase above 65 °C. Therefore it can be concluded that the mesophase is lamellar. The layer spacing is 51 Å, which means that the molecules are tilted about 43° (assuming a molecular length of 70 Å in the most extended configuration and using MM2 force field modeling). Below this temperature the material is no longer fluid but the diffuse peak still remains. This fact indicates a glassy nature of this phase. The glassy state has been observed to relax into a crystalline phase after several days.

After applying an electric field in the mesophase above a threshold of 12 V μm^{-1}, the texture becomes gradually birefringent. Under a square-wave electric field, the texture is initially grainy and bright yellow. After several seconds it gradually turns into darker green domains. In Fig. 2(a) both kinds of textures appear coexisting. After removing the electric field the isotropic black texture is no longer recovered. Yellow domains relax into a greenish gray texture whereas dark green ones become pale green [Fig. 2(b)]. This behavior can be interpreted as a field-induced flattening of the bent layers in the dark phase. In this particular case, the change is irreversible, probably due to surface effects, although the dark phase is recovered after heating the sample to the isotropic phase and cooling it down again. This behavior has been also reported in other bent-core materials [11,12]

The bright texture in Fig. 2(a) is highly birefringent and extinctions (hardly visible in the figure due to its low magnification) change with the field polarity which implies a homochiral synclinic (SmC_SP_F) arrangement under field. On the contrary the dark green texture is compatible with a racemic anticlinic structure (SmC_AP_F). Both textures relax, after field removal, into SmC_AP_A and SmC_SP_A, respectively.

It must be mentioned that under a triangular-wave electric field the homochiral structure can be recovered. In this respect, chirality changes induced by the electric field wave form have been previously reported in Ref. [13]. However, in that work the behavior was the opposite we have found here, since the triangular-wave electric field favored the racemic state, whereas the square-wave induced the homochiral state.

It must be also pointed out that the homochiral state presents very small domain size, which gives rise to a very low birefringence in the ground state. As a consequence chiral domains can be observed when uncrossing the polarizers [see Figs. 3(a) and 3(b)].

Optical activity can also be observed as we enter the mesophase from the isotropic state with the field on. Large chiral domains are clearly visible against a dark background before the birefringent texture grows over them as the temperature goes down (Fig. 4). Therefore it can be concluded that the field is responsible for the segregation of domains with different chirality, as reported in a previous work for another bent-core liquid crystal [14].

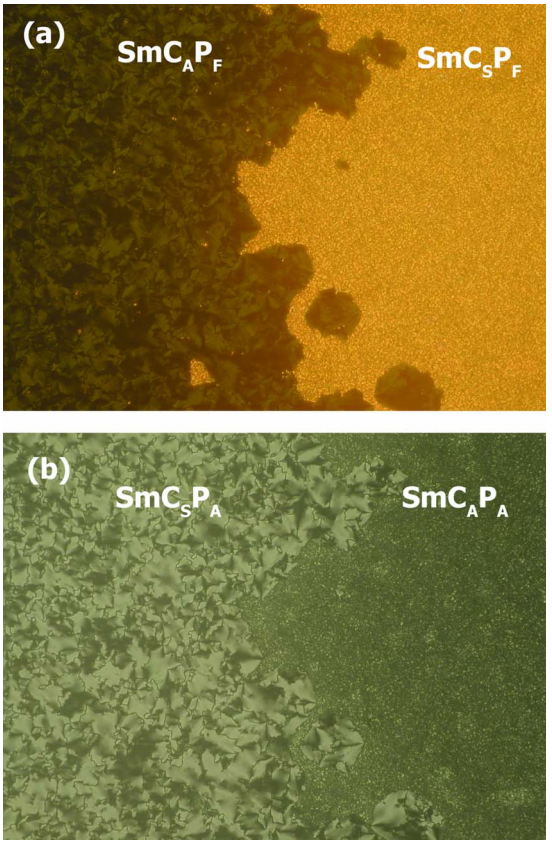

FIG. 2. (Color online) Optical textures of compound I after electric field application at 110 °C, (a) (600 μm wide) with the field on (20 V μm^{-1}) and (b) (600 μm wide) once the field is removed. In both pictures racemic and homochiral states are coexisting.

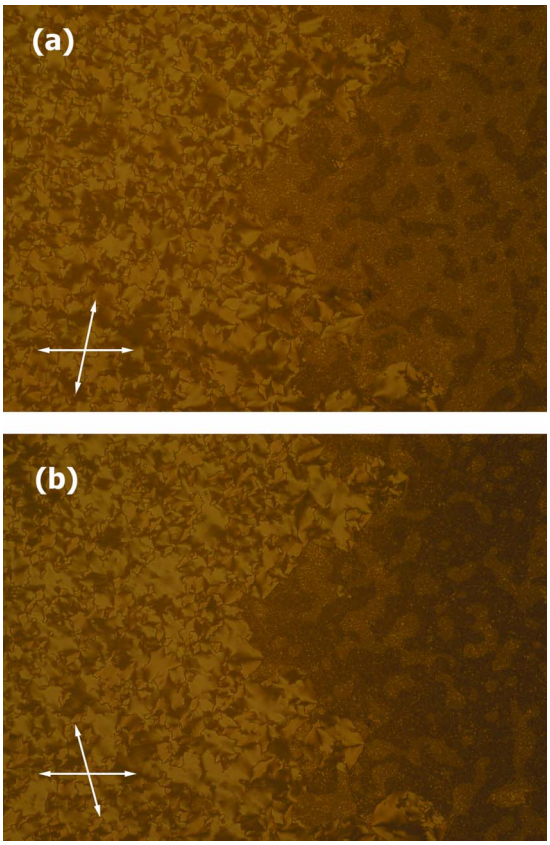

FIG. 3. (Color online) Chiral domains of the homochiral phase (right side) coexisting with racemic domains (left side) of compound I at 110 °C. The optical activity can be observed due to the small domain size in the homochiral phase, which gives rise to an almost optically isotropic texture without electric field. In (a) and (b) polarizers are slightly uncrossed in both senses (both pictures 600 μm wide).

SHG measurements confirmed the antiferroelectric character for the ground state: null signal without field and nonzero with the field on. However, the polarization switching current under a triangular-wave voltage shows only one peak per half cycle [9] (polarization about 400 nC cm^{-2}). This behavior is due to the effect of the surface pinning on the dynamic response of the material. Furthermore, compared with other bent-core liquid crystals [15], the saturated signal (with 30 V μm^{-1}) is about five times higher (as well as in compound II). Assuming that the sample is formed by a random distribution of domains whose size is smaller than the SHG coherence length, the second order dielectric susceptibility components d can be roughly estimated to be about twice those of 1,3–phenylene bis [4–(4–*n*-octyloxyphenyliminomethyl)benzoate (P-8-O-PIMB) [16]. Taking into account that the molecules have only one active leg possessing a TTF group, the synthetic strategy of using such units can give rise to materials with even higher nonlinear optical efficiencies. For example, a similar bent-core molecule with a TTF group in each leg would double the d values, i.e., four times those of the P-8-OPIMB. Using the data of the latter, found in [16], we would obtain really remarkable d coefficients of about 20 pm V^{-1}. This proves the validity of the TTF donor group as a good choice to enhance the nonlinear optical properties in this kind of materials, although the π system is not optimized in the present molecules since the ester group breaks the conjugation. The high threshold electric field prevented us from carrying out a more accurate SHG efficiency characterization in aligned samples [16] and even a rough estimation for compound III (see below).

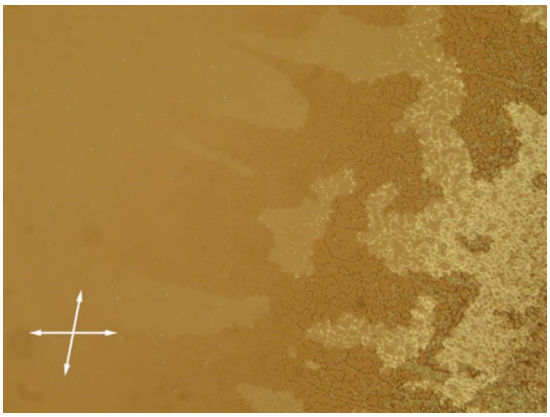

FIG. 4. (Color online) Large chiral domains are visible at 156 °C on cooling from the isotropic phase with the electric field applied (12 V μm^{-1}) by uncrossing the polarizers (1200 μm wide).

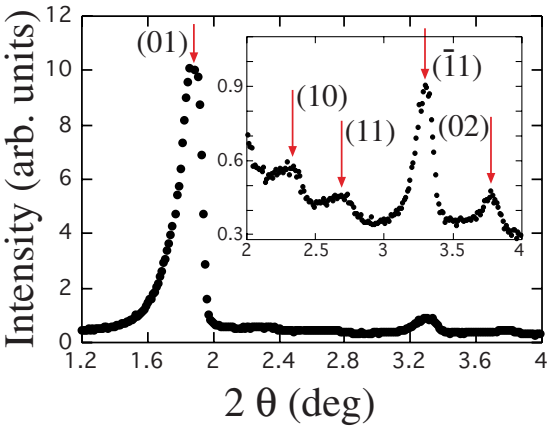

FIG. 5. (Color online) X-ray diffraction pattern of compound II at 105 °C, together with the peak indexation proposed. Intensity is plotted against 2θ, where θ is the Bragg angle. The inset shows an enlarged view of the small peaks appearing to the right of the largest one. Arrows indicate the theoretical positions of the maxima.

Photosensitivity due to the TTF units has been also found in this material. Upon illumination with uv-vis light, the conductivity increases greatly in the mesophase. Furthermore, light induces a phase transition near the clearing point and somehow alters the properties of the material at the irradiated zone. These issues have been discussed in detail in [17].

B. Compound II

Figure 5 represents the small-angle x-ray diffraction diagram obtained at 110 °C on cooling. The indexing of the pattern was carried out on the basis of an oblique two-dimensional (2D) lattice, the cell parameters being a=39 Å,

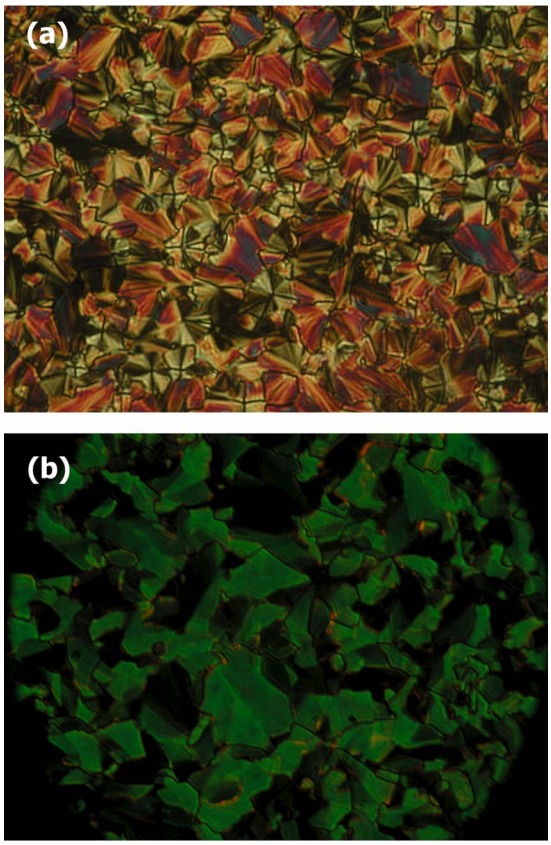

FIG. 6. (Color online) Optical textures of compound II at 105 °C: (a) (240 μm wide) on cooling from the isotropic phase and (b) (200 μm wide) after applying the electric field (20 V μm^{-1}). Once the field is applied, the texture is the same as (b) with or without field.

c=48 Å, and β=78°. The validity of the indexing scheme was checked at different temperatures on heating and cooling. A continuous variation of the lattice parameters was detected, β reduces in 2° at 95 °C. The high intensity of the peak indexed as (01) suggests a strong lamellar character. From its corresponding periodicity, a tilt of 46° is obtained if a molecular length of 67 Å deduced from molecular modeling in an all-trans conformation is assumed.

The optical textures observed during the electro-optical studies for this material are shown in Fig. 6. On cooling from the isotropic state a texture possessing pale colors with birefringence between 0.04 (greenish yellow) and 0.10 (brownish orange) is obtained [Fig. 6(a)]. If a large electric field is applied (30 V μm^{-1}, 10 Hz, square wave) the texture becomes green [Fig. 6(b)] with Δn=0.14. It is to be stressed that no optical switching is observable while a polarization current is detected (two current peaks per half cycle of the triangular-wave voltage [9]), and the green texture remains after the field is removed. Furthermore, SHG is detected only when the field is on, indicating that the material is ferroelectric under field and antiferroelectric without field. Consequently, the lack of optical switching means that the polarization inversion occurs through molecular rotations about their long axes (chiral switching). The high birefringence of the texture in Fig. 6(b) indicates that the arrangement is synclinic (both in the ground and in ferroelectric states). Therefore Fig. 6(a) corresponds to a disordered bulk where the molecular dipoles are mainly parallel to the glass plates. Then, the field effect is just to rearrange the structure by orienting the dipoles in the direction perpendicular to the glasses with the consequent increase of Δn [Fig. 6(b)]. A similar electro-optic effect has been previously reported in columnar phases of other bent-core materials [18,19]. In the present case, after the molecular reorientation, no electro-optic effect is further detected, even if the field is removed.

We propose now a structural model for the mesophase of our material. First we analyze and choose the appropriate 2D electron density distributions among those in agreement with the observed x-ray diagram. The method is standard in the crystallography of solids and has been also used in 2D [20,21] and 3D [22] liquid crystal phases before. Then, molecular cores are to be positioned on the maximum density regions of the map in order to pack and fill the volume as well as possible. This is done in agreement with previous experimental information (antiferroelectric and synclinic character in this case), and attending to packing conditions, molecular size, and optimization of steric interactions.

The periodic electron density $\rho(x,z)$ can be expanded in terms of the hl Fourier components with amplitudes given by the complex structure factor $F(h,l)$ [20]:

$$\rho(x,z) = \frac{F(00)}{A} + \frac{1}{A}\sum_{hl} \pm |F(hl)|\cos[2\pi(hx+lz)], \quad (1)$$

where A is the area of the unit cell. In the above expression we have assumed that $\rho(x,z)=\rho(-x,-z)$ for an appropriate cell origin. It can be shown that this can be done for practically the whole set of structural models proposed up to now. Under this condition the structure factor is real and, therefore $F(hl)=F(\overline{hl})$. The quantities $|F(hl)|$ are related to the hl reflection intensities as $I(hl)=|F(hl)|^2$. The intensities $I(hl)$ are obtained from the x-ray diffraction peaks after background subtraction, taking into account the Lorentz factor correction and the multiplicity of each reflection. The uncertainty left by the possible sign combinations is overcome in terms of the plausibility of the electron density maps obtained for each one. In the case of this compound, the density maps obtained for any of the sign combinations are very similar to that shown in Fig. 7. The lamellar character and a modulation of the electronic density are clearly present. The combination of signs was chosen in order to maximize the length of the white areas in the map, where the electronic density is higher, with the aim of allowing suitable molecular packing and reducing empty regions as much as possible. Figure 8(a) represents a possible structural model for the mesophase. Molecular directors have been set in such a way that are compatible with the observed optical tilt and almost perpendicularly to the longest direction of the brighter areas in the map of Fig. 7. This arrangement permits one to obtain the best packing. The phase resembles a SmC_SP_A phase undulated according to a sawtooth wave. The structure is racemic since it is synclinic antiferroelectric, therefore blue and red molecules must be present in equal proportion. It is important to point out that, as the phase is not strictly smectic, the

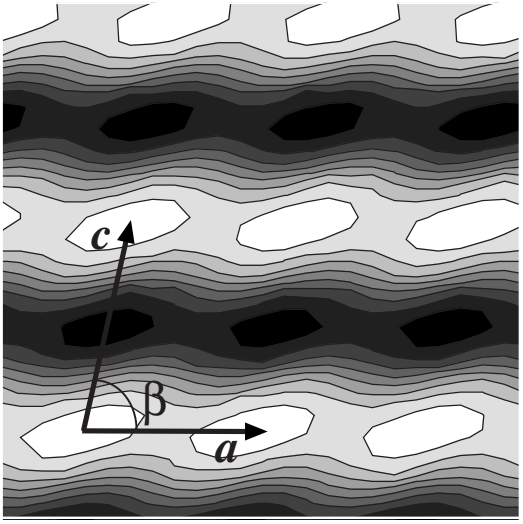

FIG. 7. 2D electron density map calculated from the data of Fig. 5 for compound II. The brighter regions represent the areas of higher electron density. In this particular case the signs chosen in Eq. (1) for the structure factors are (−−−−+). The order of signs corresponds to the appearance of the peaks in Fig. 5. The unit cell parameters are also sketched on it.

tilt angle must be understood as the angle of the molecular director with respect to the (001) direction, i.e., perpendicular to *a* vector in Fig. 7. Another alternative possibility to Fig. 8(a) is a racemic synclinic organization but with the polarity reversing now along the *a* direction. This has the advantage that the aromatic rodlike wings become aligned

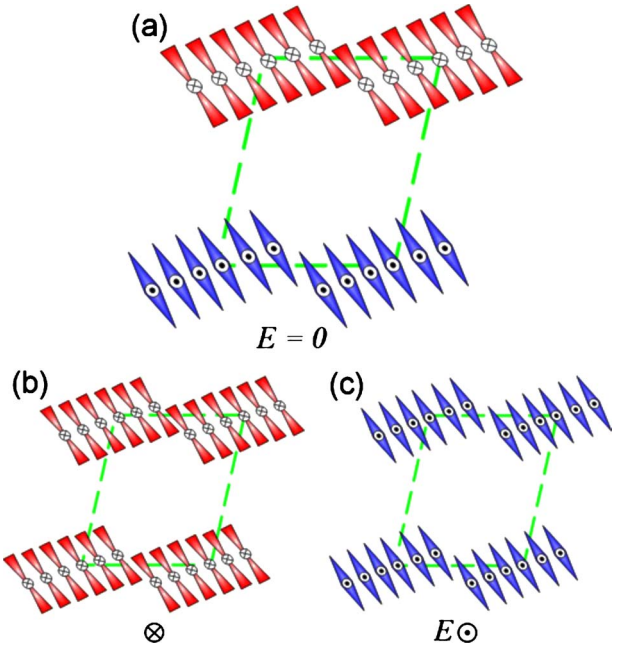

FIG. 8. (Color online) (a) Arrangement of the molecules proposed for compound II together with the corresponding structures (b) and (c) under field. The molecular packing is in agreement with the electron density in Fig. 7. The antiferroelectric ordering of the dipoles is based on the SHG measurements, but their exact distribution is unknown.

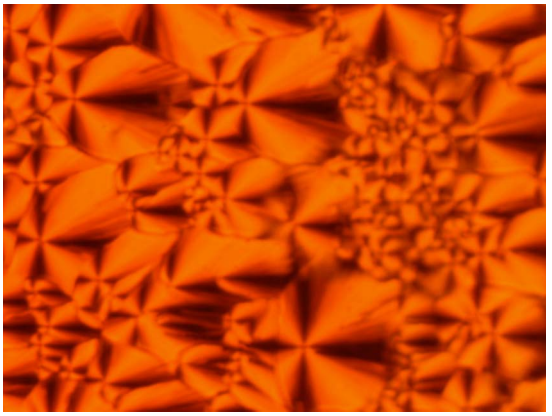

FIG. 9. (Color online) Optical texture of compound III at 163 °C on cooling from the isotropic phase with the sample between two glass slides. The red color is due to the absorption of the compound. Picture is 240 μm wide.

parallel at the edge of the blocks and this is expected to have lower energy (see, e.g., Fig. 18 in Ref. [23]). With conventional nonresonant x-ray diffraction these alternatives cannot be distinguished.

Finally, Figs. 8(b) and 8(c) illustrate the chiral switching mechanism under inversion of the electric field polarity: red molecules become blue or vice versa. The three structures in Fig. 8 are optically indistinguishable, and correspond to the texture in Fig. 6(b).

C. Compound III

On cooling this compound from the isotropic phase the texture shown in Fig. 9 is obtained. Circular domains with the extinction crosses parallel to the polarizers are observed, pointing towards an anticlinic order of the molecules in the mesophase. This texture is maintained down to room temperature. Upon application of a large electric field (20 V μm^{-1}) the birefringence increases somewhat but no appreciable switching is observed. The sample degrades if larger fields are applied.

Small angle x-ray diffraction experiments were also performed in this compound. Figure 10 shows the diffraction profile at 138 °C. Four peaks are unambiguously detected, and a small hump also appears by the side of the largest one. All of them were indexed using a simple two-dimensional rectangular lattice with cell parameters $a=141$ Å and $c=52$ Å. No substantial changes were observed at other temperatures within the mesophase, indicating that the rectangular geometry of the lattice is not accidental. Therefore the symmetry of the structure is orthorhombic, which implies an anticlinic molecular arrangement (a synclinic arrangement is always monoclinic). Modeling the molecule in an all-trans conformation, a molecular length of 82 Å is obtained and the resulting tilt is 51°. This tilt angle and the anticlinic order should give a low value for the birefringence, so the reddish color in Fig. 9 is mainly attributed to the large absorption of the material in the blue region. The fact that the peak indexed as (01) is the largest strongly suggests a lamellar character.

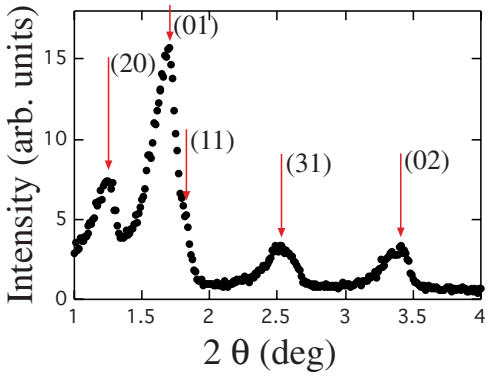

FIG. 10. (Color online) X-ray diffraction pattern of compound III at 138 °C, together with the peak indexation proposed. Intensity is plotted against 2θ, where θ is the Bragg angle. Arrows indicate the theoretical positions of the maxima.

SHG measurements were also performed, but no signal was detected even with a large field applied (20 V μm^{-1}). Therefore fields below the threshold for the dielectric rupture (about 25 V μm^{-1}) are not enough to induce the ferroelectric order.

We propose now a structural model for this mesophase using the same procedure as for compound II. The rectangular symmetry of the electron density map and the existence of the (01) reflection restrict the possible plane groups of the density map to $pm2m$ and $pm2g$ [24]. These symmetries imply the two following possible relations among the structure factors: $F(hl)=F(\bar{h}l)$ or $F(hl)=(-1)^h F(\bar{h}l)$, respectively [20]. Many of the sign combinations in Eq. (1) produce the same density maps with shifts in the origin of the coordinate system. This fact leaves only a few different possibilities. Examining the electron density graphical representations obtained for the different sign choices, we can discard those possessing a nonlamellar character or layer structures with narrow electron density rich areas. Taking those facts into account one ends up with the possibility shown in Fig. 11. A clear modulation of the layer density is noticeable. One peculiar feature of the density map is the existence of two maxima per molecular core. This can be understood as being originated by the two TTF groups at the end of the core, which are by far the molecular parts with the highest electron density. This characteristic is very unusual and is due to the

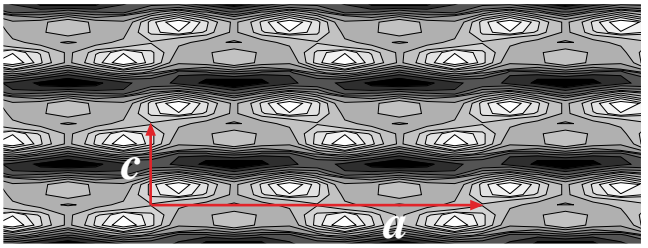

FIG. 11. (Color online) 2D electron density map calculated from the data of Fig. 10 for compound III and unit cell parameters. The brighter regions represent the areas of higher electron density. The signs chosen in Eq. (1) for the structure factors are (+−−−−). The order of signs corresponds to the appearance of the peaks in Fig. 10.

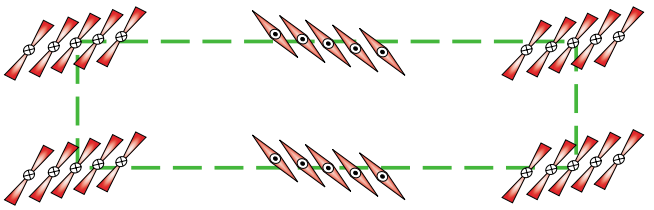

FIG. 12. (Color online) Arrangement of the molecules proposed for compound III. The molecular packing is in agreement with the electron density in Fig. 11. The antiferroelectric ordering of the dipoles is based on the SHG measurements, but their exact distribution is unknown.

especial molecular chemical structure. In addition, the positions of the two maxima determine the molecular orientation, which is compatible with the anticlinic arrangement and with the magnitude of the tilt angle calculated above. A plausible arrangement of the molecules in this phase is sketched in Fig. 12. The proposed structure implies the existence of defect regions to accommodate molecules with opposite tilt. The higher disorder expected in these areas diminishes the effective charge density corresponding to the TTF groups. It is difficult to determine the precise molecular arrangement at the defects but probably the connections at these regions are achieved through splay of the polarization [25].

It is interesting to compare this map with that of compound II, where the double maximum per molecular core is not visible. From a mere experimental viewpoint this fact occurs because of the small size of the (02) reflection (see Fig. 5) in comparison with the corresponding peak in compound III (last maximum of Fig. 10). In compound II there is only one electron-rich group per molecule and this implies on the one hand a smaller average electronic density; but, on the other hand and more importantly, it also gives rise to a larger disorder in the smectic layer since two TTF groups per molecule (compound III) permit a better orbital overlap in neighboring molecules and lead to a more efficient molecular packing through the connection between TTF groups. As a consequence the electron-rich region is smeared out in the map of compound II but is clearly visible in the present case.

The structure in Fig. 12 is not the unique possibility but it is certainly one of the simplest. The phase would be homochiral and antiferroelectric. Essentially, the structure is an undulated SmCP (USmCP) phase and the modulation within a layer can be understood as due to a packing fault or defect where the density is smaller than in the rest of the layer. The defects would occur at the crests and troughs of the undulation [26]. This molecular organization corresponds to the so-called $SmCPU_A[S]$ structure as defined in Ref. [27]. Here U means undulation, A indicates opposite slopes in adjacent stripes, and [S] denotes that adjacent stripes have the same chirality. Other possible arrangements compatible with the x-ray and SHG data are the antiferrolectric racemic $SmCPU_A[S,A]$ structures (two kinds of defects between adjacent stripes, one with the same chirality and one with the opposite chirality in successive stripes).

Since the tilt alternates along the layer and not between consecutive layers (as in the traditional SmC_AP_A) it seems that the switching should be strongly hindered. This is in fact

experimentally observed since the material undergoes dielectric breakdown before showing any switching.

Finally it is worth mentioning the unusually small enthalpy associated with the mesophase-isotropic liquid transition (see Fig. 1). We do not know the reasons for this peculiar property of the material. Anyway, this small enthalpy is compatible with the existence of an important amount of cybotactic groups in the isotropic phase. These smectic clusters were evidenced by x-ray measurements, which revealed an abnormal persistence of a broadened smectic peak several degrees above the clearing point.

IV. CONCLUSIONS

Three bent-core liquid crystals with TTF units in their lateral structures have been studied. Three different mesophases have been found: a lamellar optically isotropic phase, a two-dimensional oblique phase, and a two-dimensional rectangular phase, the last two with a high degree of "lamellarization." The first one undergoes a transition to a SmCP phase above a threshold electric field. For compounds II and III structural models have been deduced from the electronic density distributions obtained by using the intensities of the x-ray reflection peaks. According to the SHG results, the ground state of the three materials is clearly antiferroelectric. Furthermore, the SHG efficiency of compounds I and II under field is rather good, confirming that the TTF units work satisfactorily as donor groups in bent-core molecules.

ACKNOWLEDGMENTS

Three of us (J.M.P., I.A., and I.C.P.) thank the Basque Government, the MEC of Spain, and the Aragón Government, respectively, for a grant. This work was supported by the CICYT-FEDER of Spain-EU (Project No. MAT2006-13571-C02) and the Aragón Government.

[1] T. Niori, T. Sekine, J. Watanabe, T. Furukawa, and H. Takezoe, J. Mater. Chem. **6**, 1231 (1996).
[2] G. Pelzl, S. Diele, and W. Weissflog, Adv. Mater. (Weinheim, Ger.) **11**, 707 (1999).
[3] H. Takezoe and Y. Takanishi, Jpn. J. Appl. Phys., Part 1 **45**, 597 (2006).
[4] R. A. Reddy and C. Tschierske, J. Mater. Chem. **16**, 907 (2006).
[5] J. L. Segura and N. Martín, Angew. Chem., Int. Ed. **40**, 1372 (2001).
[6] M. R. J. Bryce, Chem. Soc. Rev. **20**, 355 (1991); N. S. Nalwa, *Handbook of Organic Conductive Molecules and Polymers* (Wiley, New York, 1997), Vol. 1; M. R. J. Bryce, J. Mater. Chem. **10**, 589 (2000); Chem. Rev. (Washington, D.C.) **104**, 4887 (2004).
[7] M. Mas-Torrent and C. Rovira, J. Mater. Chem. **16**, 433 (2006); E. Gomar-Nadal, J. Puigmartí-Luis, and D. B. Amabilino, Chem. Soc. Rev. **37**, 490 (2008).
[8] J. Casado, M. Zgierski, M. C. Ruiz Delgado, J. T. López Navarrete, M. Mas-Torrent, and C. Rovira, J. Phys. Chem. C **111**, 10110 (2007).
[9] I. C. Pintre, J. L. Serrano, M. B. Ros, J. Ortega, I. Alonso, J. Martinez-Perdiguero, C. L. Folcia, J. Etxebarria, F. Goc, D. B. Amabilino, J. Puigmarti-Luis, and E. Gomar-Nadal, Chem. Commun. (Cambridge) **22**, 2523 (2008).
[10] N. Pereda, C. L. Folcia, J. Etxebarria, J. Ortega, and M. B. Ros, Liq. Cryst. **24**, 451 (1998).
[11] C. Keith, R. A. Reddy, A. Hanser, U. Baumeister, and C. Tschierske, J. Am. Chem. Soc. **128**, 3051 (2006).
[12] J. Ortega, C. L. Folcia, J. Etxebarria, N. Gimeno, and M. B. Ros, Phys. Rev. E **68**, 011707 (2003).
[13] G. Heppke, A. Jàkli, S. Rauch, and H. Sawade, Phys. Rev. E **60**, 5575 (1999).
[14] J. Martínez-Perdiguero, I. Alonso, C. L. Folcia, J. Etxebarria, and J. Ortega, Phys. Rev. E **74**, 031701 (2006).
[15] I. C. Pintre, N. Gimeno, J. L. Serrano, M. B. Ros, I. Alonso, C. L. Folcia, J. Ortega, and J. Etxebarria, J. Mater. Chem. **17**, 2219 (2007).
[16] J. Ortega, J. Gallastegi, C. L. Folcia, J. Etxebarria, N. Gimeno, and M. B. Ros, Liq. Cryst. **31**, 579 (2004).
[17] J. Martínez-Perdiguero, I. Alonso, J. Ortega, C. L. Folcia, J. Etxebarria, I. C. Pintre, M. B. Ros, and D. B. Amabilino, Phys. Rev. E **77**, 020701(R) (2008).
[18] J. Ortega, M. R. de la Fuente, J. Etxebarria, C. L. Folcia, S. Díez, J. A. Gallastegui, N. Gimeno, M. B. Ros, and M. A. Perez-Jubindo, Phys. Rev. E **69**, 011703 (2004).
[19] J. Szydlowska, J. Mieczkowski, J. Matraszek, D. W. Bruce, E. Gorecka, D. Pociecha, and D. Guillon, Phys. Rev. E **67**, 031702 (2003).
[20] C. L. Folcia, I. Alonso, J. Ortega, J. Etxebarria, I. Pintre, and M. B. Ros, Chem. Mater. **18**, 4617 (2006).
[21] E. Gorecka, N. Vaupotic, and D. Pociecha, Chem. Mater. **19**, 3027 (2007).
[22] X. Zeng, G. Ungar, and M. Impéror-Clerc, Nature Mater. **4**, 562 (2005).
[23] C. Keith, G. Dantlgraber, R. A. Reddy, U. Baumeister, and C. Tschierske, Chem. Mater. **19**, 694 (2007).
[24] *International Tables for Crystallography, Subperiodic Groups*, edited by V. Kopsky and D. B. Litvin (Kluwer Academic, Dordrecht, 2002), Vol. E.
[25] N. Vaupotic, M. Copic, E. Gorecka, and D. Pociecha, Phys. Rev. Lett. **98**, 247802 (2007).
[26] D. A. Coleman, J. Fernsler, N. Chattham, M. Nakata, Y. Takanishi, E. Körblova, D. R. Link, R.-F. Shao, W. G. Jang, J. E. Maclennan, O. Mondainn-Monval, C. Boyer, W. Weissflog, G. Pelzl, L.-C. Chien, J. Zasadzinski, J. Watanabe, D. M. Walba, H. Takezoe, and N. A. Clark, Science **301**, 1204 (2003).
[27] D. A. Coleman, C. D. Jones, M. Nakata, N. A. Clark, D. M. Walba, W. Weissflog, K. Fodor-Csorba, J. Watanabe, V. Novotna, and V. Hamplova, Phys. Rev. E **77**, 021703 (2008).